Synthesis and Characterization of Technetium-99m-Labeled Tropanes as Dopamine Transporter-Imaging Agents

Sanath K. Meegalla,[†] Karl Plössl,[†] Mei-Ping Kung,[†] Sumalee Chumpradit,[†] D. Andrew Stevenson,[†] Steven A. Kushner,[†] William T. McElgin,[‡] P. David Mozley,[†] and Hank F. Kung*[,†,§]

Departments of Radiology, Pharmacology, and Psychiatry, University of Pennsylvania, 3700 Market Street, Philadelphia, Pennsylvania 19104

Received July 23, 1996[⊗]

In the development of novel Tc-99m-labeled tropane derivatives as dopamine transporter (reuptake site)-imaging agents, a series of neutral and lipophilic complexes containing bis(aminoethanethiol) as a neutral complexing moiety for a [^{99m}Tc]TcO^{3+} center core was successfully prepared. Biological evaluation of the Tc-99m-labeled complexes **13**−**16** as central nervous system (CNS) dopamine transporter-imaging agents was reported. Synthesis of the tropane derivatives was achieved by stepwise reactions adding two aminoethanethiol units. The final free thiol ligands were obtained by deblocking the 4-methoxybenzyl protecting group with $Hg(OAc)_2$ to obtain trifluoroacetate salts. All of the Tc-99m complexes, with the exception of **16**, displayed good initial brain uptake and selective uptake in the striatal area, where dopamine transporters are concentrated. One of the compounds, [2-[[2-[[[3-(4-chlorophenyl)-8-methyl-8-azabicyclo[3.2.1]oct-2-yl]methyl](2-mercaptoethyl)amino]ethyl]amino]ethanethiolato-(3−)-*N*2,*N*2′,*S*2,*S*2′]oxo-[1*R*-(*exo*-*exo*)]- [^{99m}Tc]technetium, [^{99m}Tc]TRODAT-1 (**13**), displayed the highest initial uptake in rat brain (0.4% at 2 min post iv injection); the striatal/cerebellar (ST/CB) ratio reached 2.8 at 60 min after an iv injection. The specific uptake in rat brain can be blocked by pretreating rats with a competing dopamine transporter binding agent, β-CIT (RTI-55, 2β-carbomethoxy-3β-(4-iodophenyl)tropane; iv, 1 mg/kg), which reduced the regional brain uptake ratio (ST/CB) to 1.2. In contrast, the specific striatal uptake was not affected by pretreating rats with a noncompeting ligand, haldol (iv, 1 mg/kg). After an iv injection of 9 mCi of [^{99m}Tc]TRODAT-1 (**13**), *in vivo* images of baboon brain using single-photon emission-computed tomography exhibited excellent localization in striatum (basal ganglia), where dopamine neurons are known to be concentrated. This series of compounds may provide a convenient source of short-lived imaging agents for routine diagnosis of CNS diseases (i.e., Parkinson's disease) in which changes in the dopamine transporter concentration are implicated.

Introduction

Recently, a large number of dopamine transporter (reuptake site)-imaging agents based on cocaine or its closely related congeners, tropane derivatives, have been reported.[1−4] The regional brain distribution of cocaine is largely concentrated in the basal ganglia, where dopamine neurons are located. [^{11}C]*N*-Methyl-labeled cocaine[5,6] is a very useful PET (positron emission tomography) ligand for studying the pharmacology and drug effects of cocaine itself; however, additional modifications of the cocaine molecule have led to the development of PET imaging agents such as CFT[7−9] (*N*-methyl-2β-carbomethoxy-3β-(4-fluorophenyl)tropane, WIN35,428) and single-photon emission-computed tomography (SPECT) imaging agents β-CIT[10−13] (*N*-methyl-2β-carbomethoxy-3β-(4-iodophenyl)tropane), IPT[14] (*N*-(3-iodopropen-2-yl)-2β-carbomethoxy-3β-(4-chlorophenyl)tropane), FP-CIT[15] (*N*-(3-fluoropropyl)-2β-carbomethoxy-3β-(4-iodophenyl)tropane), and other related derivatives that display much higher binding affinity and selectivity to dopamine transporters. These PET and SPECT imaging agents displayed excellent specific uptake in the striatum (basal ganglia) area and are more suitable than GBR12,935[16] for imaging dopamine transporters. The dopamine transporter ligands are useful in evaluating changes in dopamine transporters *in vivo* and *in vitro*, especially for patients with Parkinson's disease (PD), which is characterized by a selective loss of dopamine neurons in the basal ganglia and substantia nigra. Recent publications describing the use of [^{11}C]CFT[7] (WIN35,428) and [^{123}I]β-CIT[10,17] suggest a strong correlation between the decrease in the localization of dopamine transporter ligands in the anterior putamen area and PD symptoms.[7,8,17] The results provide an impetus toward the further development of these agents for diagnosing and monitoring the treatment of PD patients. Currently, [^{123}I]β-CIT is being widely investigated for this purpose. However, one of the drawbacks of [^{123}I]β-CIT is the time required (>18 h) for reaching an optimal uptake ratio in the target area, the basal ganglia (BG), vs the nontarget area, the frontal cortex (CX). Because of the need for agents with faster equilibrium times, new ligands, such as [^{123}I]IPT[14,18−20] and [^{123}I]FP-CIT,[13,15] both of which reach maximum uptake in human brain within a few hours, will play an important future role as the agents of choice.

Technetium-99m ($t_{1/2}$ = 6 h, 140 keV) is the most commonly used radionuclide in diagnostic nuclear medicine.[21,22] Its popularity is mainly due to the fact that the radionuclide can be readily produced by a Mo-99/Tc-99m generator, the medium γ-ray energy emitted by

* Corresponding author: Hank F. Kung, Ph.D., 3700 Market St, Room 305, Philadelphia, PA 19104. Tel: (215)662-3096. Fax: (215)-349-5035. E-mail: kunghf@sunmac.spect.upenn.edu.
[†] Department of Radiology.
[‡] Department of Psychiatry.
[§] Department of Pharmacology.
[⊗] Abstract published in *Advance ACS Abstracts,* December 15, 1996.

S0022-2623(96)00532-8 CCC: $14.00

Tc-99m (140 keV) is suitable for γ-camera detection, and the physical half-life is often compatible with the biological localization and residence time required for imaging. Currently, about 85% of routine nuclear medicine procedures are performed with radiopharmaceuticals based on Tc-99m. In the past 10 years, significant progress has been made on the chemistry of technetium, using the chemical level of Tc-99 ($t_{1/2} = 2.1 \times 10^5$ years).[21] Improvements in the understanding of technetium chemistry have significantly enhanced the development of a new generation of technetium radiopharmaceuticals for clinical use and potentially will benefit millions of patients who receive Tc-99m agents for routine nuclear medicine diagnosis. It is well established that when [^{99m}Tc]pertechnetate (TcO_4^-), the most commonly available starting material, is reduced by a reducing agent, such as stannous chloride, in the presence of "soft" chelating ligands, including N_2S_2 and NS_3, $[Tc^vO]^{3+}N_2S_2$ or $[Tc^vO]^{3+}NS_3$ complexes are formed. Several recent reports demonstrate that it is possible to incorporate $[Tc^vO]^{3+}N_2S_2$ into potential receptor-selective imaging agents for muscarinic receptors,[23] vesamicol sites,[24] and steroid hormone receptors.[25−30] The use of other chelating agents for preparing Tc-99m muscarinic receptor-imaging agents has also been reported.[31] However, all of these central nervous system (CNS) receptor-specific Tc-99m imaging agents have demonstrated limited success in *in vivo* studies.

Recently, a series of neutral and lipophilic complexes, containing *N*-(alkylthiolato)tropane, aminobis(ethylthiolato), and a [^{99m}Tc]TcO^{3+} center core, was prepared and evaluated as CNS dopamine transporter-imaging agents in rats.[32] One of the compounds, [methyl 3-(4-chlorophenyl)-8-(2-mercaptoethyl)-8-azabicyclo[3.2.1]octane-2-carboxylato-*S*][2,2′-(methylimino)bis[ethanethiolato]]-(2−)-*N*,*S*,*S*′]oxo[^{99m}Tc]technetium, displayed low initial uptake in rat brain (0.1% at 2 min post iv injection), but the striatal/cerebellar (ST/CB) ratio reached 3.50 at 60 min after an iv injection. The corresponding rhenium complex displayed the expected structure, containing a square-pyramidal core with the Re═O in the axial position (Figure 1).

Another related Tc-99m-labeled tropane derivative,[33] technepine, which was reported to have a high affinity to the dopamine transporter, may also be useful as an *in vivo* imaging agent. Both of the current examples of Tc-99m-labeled tropane derivatives were modified at the *N*-methyl position of the tropane ring to add a technetium-carrying moiety. In order to increase the initial brain uptake and limit the molecular size of the final Tc-99m-labeled tropane derivative, a novel series of derivatives with the bis(aminoethanethiol) ligand attached at the 2β-position was prepared. In this report, synthesis, radiolabeling, a preliminary biodistribution study of the new Tc-99m complexes in rats, and a SPECT imaging study in a baboon are described.

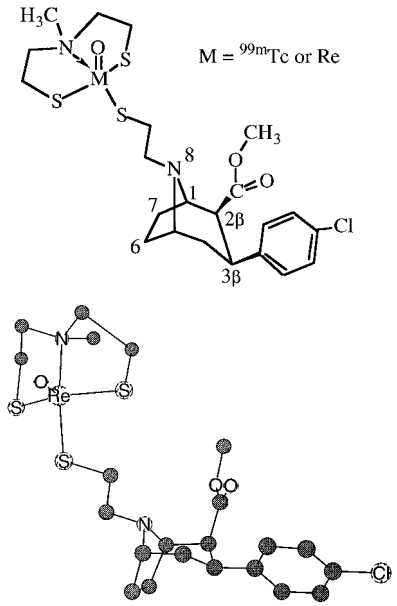

Figure 1. X-ray structure of [methyl 3-(4-chlorophenyl)-8-(2-mercaptoethyl)-8-azabicyclo[3.2.1]octane-2-carboxylato-*S*][2,2′-(methylimino)bis[ethanethiolato]](2−)-*N*,*S*,*S*′]oxorhenium.

Scheme 1

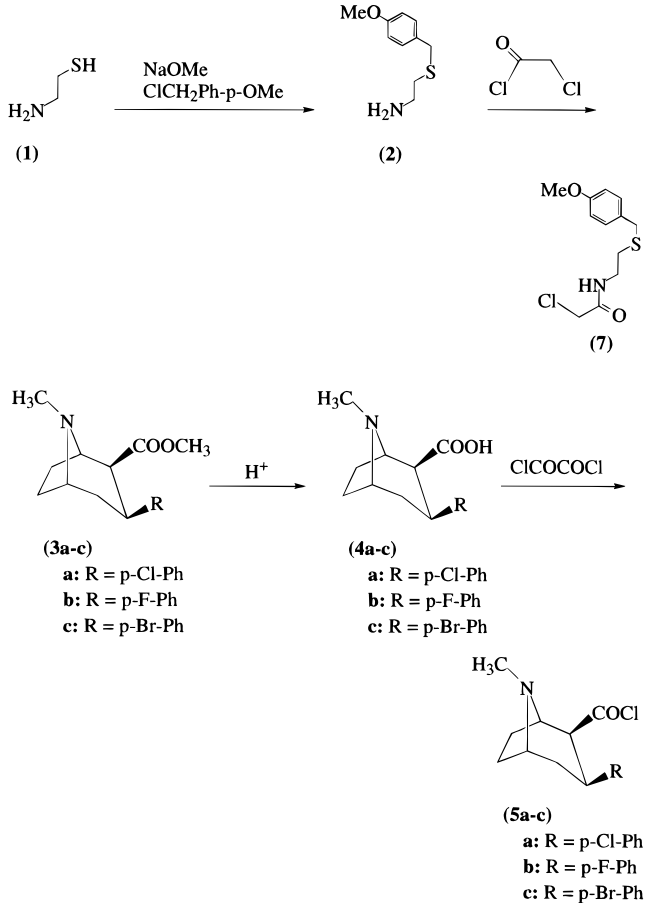

Results

Schemes 1−3 illustrate the synthetic strategy employed for the preparation of the compounds described in this paper. Syntheses of the 3β-(*p*-chloro-, *p*-fluoro-, and *p*-bromophenyl)tropane esters **3a**−**c** and the corresponding carboxylic acids **4a**−**c** were carried out according to previously reported procedures.[9,34] The corresponding acyl chlorides **5a**−**c**, which were prepared by the action of oxalyl chloride on carboxylic acids **4a**−**c** at room temperature, were not isolated but intercepted with amine **2** to obtain amides **6a**−**c**. Secondary amines **8** were prepared by diborane reduction of amides **6** and converted to amides **9** by alkylations with alkyl chloride **7**. The amide functions of compounds **9** were reduced with BH_3·THF to yield compounds **11**. Amines **11** and amide **9** were deprotected with $Hg(OAc)_2$ to obtain

Scheme 2

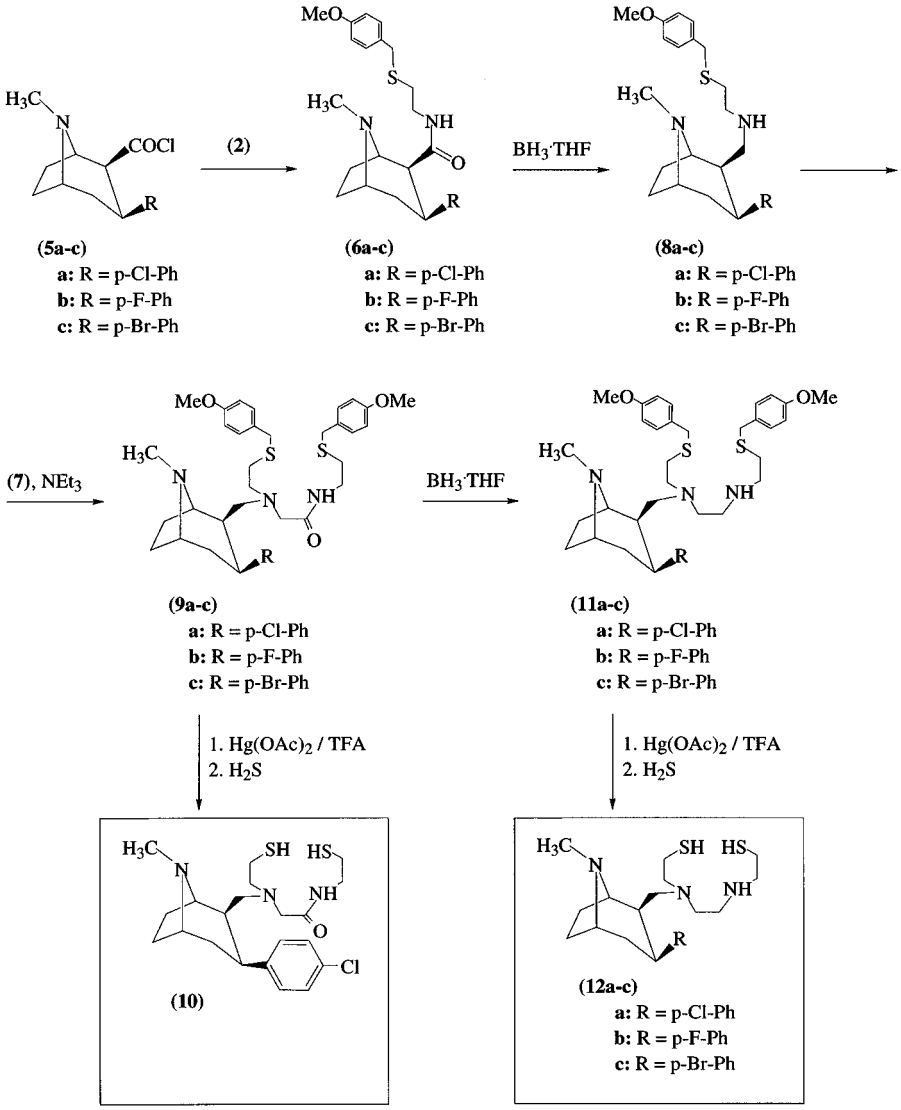

trifluoroacetate salts of dithiols **10** and **12**. Since the instability of these disulfides prevented any further purification, they were obtained as their trifluoroacetate salts and used directly without further characterization for the preparation of rhenium (**17**) and [^{99m}Tc]technetium (**13**−**16**) complexes.

Rhenium oxo complexes of bisthiols **12a**,**b** were prepared as surrogates for corresponding Tc complexes, by employing [Bu_4N][$ReOCl_4$] as a rhenium starting material in MeOH at room temperature in the presence of triethylamine as an acid scavenger. Thin layer chromatography, as well as NMR data of purified rhenium complexes, indicated that there were two isomers formed in each complexation reaction. Although the NMR spectra of the rhenium complexes were complicated due to the presence of isomers and the diastereotopic nature of all methylene protons, IR and high-resolution mass spectral data confirmed the presence of the expected rhenium oxo complexes (see Discussion and Figure 4).

The radiolabeling of **12a**−**c** and **10** with sodium [^{99m}Tc]pertechnetate was successfully achieved using stannous(II) glucoheptonate as the reducing agent to produce **13**−**16** in good yield (80%) and high radiochemical purity (>95%). Key properties for these potential dopamine transporter-imaging agents are their neutrality and lipophilicity. Tc-99m-labeled complexes **13**−**15** displayed excellent medium range lipophilicity (partition coefficients between 1-octanol and pH 7.0 buffer of 99−262). Complex **16** was an exception; it fell out of this range, with a PC of 1818 (Table 1).

Biodistribution studies of **13**−**16** in rats were performed after an iv injection of a tracer dose. The results showed a distribution pattern reflecting regional perfusion (i.e., high uptake in muscle, kidney, liver, brain and skin; Tables 1 and 2). However, the brain uptake is moderate, ranging from 0.43% to 0.11% dose/organ at 2 min for the four complexes. The complex containing an amide group, **16**, showed the lowest brain uptake (Table 1), despite its high lipophilicity (PC = 1818). The results suggest that an amide group in the technetium N_2S_2 complexing moiety may hinder the initial brain uptake.[35] Increasing the lipophilicity of these compounds does not appear to improve brain uptake in rats. The most significant finding of this initial biodistribution study is that the brain uptake of these complexes, except **16**, was highly concentrated in the striatal area, where the dopamine transporters are located, compared to a region with no dopamine neurons (i.e., the cerebellar region). At 60 min after an iv injection, the ratios of ST/CB were found to be 2.66, 2.18, and 2.82 for **13**, **14**, and **15**, respectively. However, complex **16** showed

Scheme 3

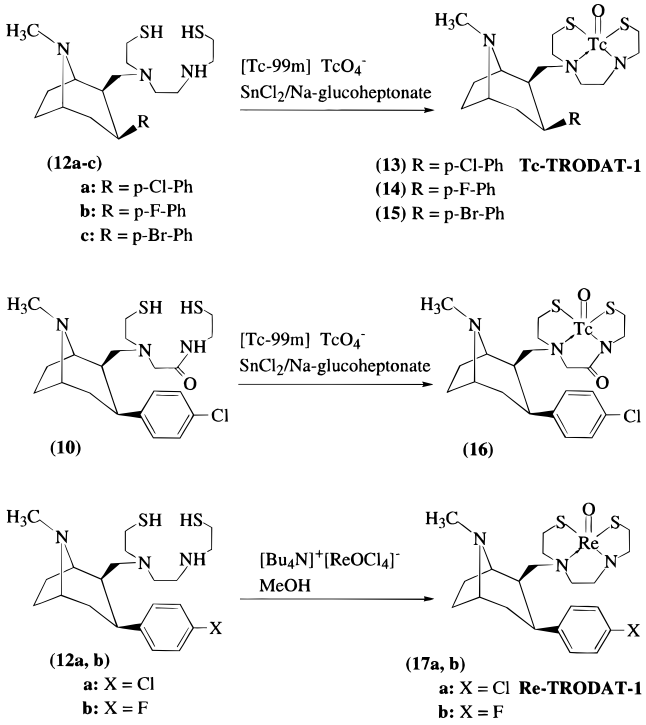

Table 1. Brain Uptake of Four [^{99m}Tc]TRODAT Derivatives (% dose/organ)

compound	2 min	60 min	ST/CB ratio at 60 min[a]	PC[b]
13, TRODAT-1	0.43 ± 0.16	0.12 ± 0.001	2.66	227
14	0.37 ± 0.09	0.098 ± 0.014	2.18	99
15	0.41 ± 0.03	0.18 ± 0.01	2.82	262
16	0.11 ± 0.02	0.07 ± 0.014[c]	1.17[c]	1818

[a] Striatum/cerebellum (ST/CB) ratio: percentage dose per gram of striatum/percentage dose per gram of cerebellum. [b] PC: measured between 1-octanol and pH 7.0 phosphate buffer. [c] Data were from rats sacrificed at 30 min.

little specific uptake (ST/CB = 1.17) at 60 min post iv injection. The initial biodistribution study in rats suggested that [^{99m}Tc]TRODAT-1 (**13**) is the best imaging agent candidate in this series of complexes. It displayed the highest initial brain uptake and high retention in the target area (i.e., striatum) at later time points; therefore, a more detailed biodistribution study was carried out.

Specific uptake of [^{99m}Tc]TRODAT-1 (**13**) at different time points displayed a prolonged retention, and the ST/CB ratio in rat brain reached a maximum value of 4.07 at 4 h after injection (Table 3). Blocking studies in rats were performed at 60 min postinjection to characterize further the uptake and binding. In this series of regional brain uptake studies in rats, the ST/CB ratio at 60 min postinjection was 2.66 (Figure 1). The specific uptake of [^{99m}Tc]TRODAT-1 (**13**) in rat striatum could be blocked by pretreating rats with a dose of β-CIT (1 mg/kg, iv), a known dopamine transporter ligand. The specific binding, as indicated by ST/CB, was reduced to 1.2 after pretreatment with β-CIT. The specific binding was not reduced by pretreatment with haldol (1 mg/kg, iv), an agent with a mixed pharmacological profile (binding to various CNS receptors, but not to the dopamine transporter); no blocking effect was observed. The ST/CB ratio (2.6) was identical with that in control rats (Figure 2). The results suggested that uptake in the rat striatum was specifically related to the dopamine transporter in rat brain.

To evaluate further the potential of [^{99m}Tc]TRODAT-1 (**13**), [2-[[2-[[[3-(4-chlorophenyl)-8-methyl-8-azabicyclo-[3.2.1]oct-2-yl]methyl](2-mercaptoethyl)amino]ethyl]amino]ethanethiolato(3−)-*N*2,*N*2′,*S*2,*S*2′]oxo-[1*R*-(*exo*-*exo*)][^{99m}Tc]technetium, as a dopamine transporter-imaging agent, a SPECT imaging study was carried out in a female baboon. To facilitate the identification of anatomical localization, the coronal, transaxial, and sagittal SPECT images (1.34 mm thick) obtained 60−90 min postinjection were coregistered with the MRI images of the same baboon (Figure 3). The fused images displayed excellent consistency with the expected localization of this agent in caudate and putamen areas, where the dopamine transporters are known to be located. The images also showed good correlation with PET imaging agent [^{11}C]CFT[7,8] and SPECT imaging agent [^{123}I]β-CIT.[10−12] *In vitro* binding studies of rhenium complex **17a** in rat striatal homogenates displayed good binding affinity (K_i = 14 nM, using [^{125}I]IPT[20] as the ligand; K_d = 0.2 nM), while the bis(ethanethiol) **12a** displayed a comparable affinity (K_i = 7 nM). Although the binding affinity of the corresponding rhenium complex **17a** is not as potent as other iodinated tropane derivatives, the brain uptake and retention of [^{99m}Tc]-TRODAT-1 (**13**) appears to be sufficient for *in vivo* SPECT imaging in nonhuman primates.

Discussion

Despite its attractive physical properties, technetium is a difficult element for designing suitable SPECT ligands. Technetium is a transition metal and requires a complexing agent to stabilize it at different valence states.[22] Valence states can vary from 7+ (as pertechnetate) to 0, depending on the reaction conditions and chelating agents used during preparation.[21] After complexation, the molecules invariably become big and bulky, which is the limiting factor in designing a molecule targeted to (a) specific biological process(es). Additional requirements for Tc-99m-labeled complexes as CNS receptor-imaging agents are (i) small (molecular weight < 750), with good lipophilicity (partition coefficient ∼ 50−1000), (ii) high binding affinity (K_i < 10 nM) and high selectivity, and (iii) ideal brain uptake in rats >0.5% dose/organ at 2 min post iv injection. This novel series of compounds differs from those previously reported in that the substitution of the bis(aminoethanethiol) ligand is attached at the 2β-position of the tropane core structure. It is apparent that by choosing this position, the corresponding Tc-99m-labeled agent displayed a 3−4-fold increase in initial brain uptake (0.1% for N-substituted compound[32] vs 0.3−0.4% in brain at 2 min postinjection) and concomitantly retained the specific uptake in the striatum area of the brain. The present observation suggests that, in this series of compounds, the 3β-*p*-fluoro is slightly less favorable than the corresponding 3β-*p*-chlorophenyl derivative. As previously reported for the same series of tropane derivatives, the 3β-*p*-fluoro derivative displayed a lower brain uptake, which may be due to its lower binding affinity to dopamine transporters.[3]

The most promising compound in this series, [^{99m}Tc]-TRODAT-1 (**13**), clearly displays the desired properties described above. Even though the initial study reported

Table 2. Biodistribution in Rats Post iv Injection of [^{99m}Tc]TRODAT Ligands[a]

organ/region	**13**	**14**	**15**	**16**
		2 min Postinjection		
blood	4.94 ± 0.46	4.15 ± 0.40	2.00 ± 0.28	5.19 ± 0.49
heart	1.47 ± 0.16	1.92 ± 0.10	1.51 ± 0.19	1.33 ± 0.09
muscle	10.84 ± 1.95	15.42 ± 5.58	13.66 ± 2.15	9.67 ± 2.44
lung	6.82 ± 0.37	11.04 ± 1.41	6.46 ± 0.35	4.56 ± 0.65
kidney	5.13 ± 0.75	6.88 ± 0.46	4.66 ± 0.64	3.46 ± 0.41
spleen	0.42 ± 0.16	0.39 ± 0.09	0.52 ± 0.15	0.94 ± 0.34
liver	16.62 ± 2.11	18.5 ± 1.70	13.75 ± 1.26	25.05 ± 4.16
skin	2.66 ± 0.35	7.37 ± 0.36	2.54 ± 0.48	3.94 ± 0.63
brain	0.43 ± 0.16	0.37 ± 0.009	0.41 ± 0.03	0.106 ± 0.018
		60 min Postinjection		
blood	2.14 ± 0.17	1.24 ± 0.17	0.92 ± 0.06	1.89 ± 0.20
heart	0.19 ± 0.02	0.71 ± 0.008	0.19 ± 0.01	0.36 ± 0.04
muscle	10.28 ± 1.36	11.07 ± 0.45	9.47 ± 1.98	14.34 ± 1.76
lung	1.86 ± 0.36	1.54 ± 0.13	1.49 ± 0.09	3.00 ± 0.38
kidney	3.06 ± 0.14	2.79 ± 0.09	1.68 ± 0.22	1.41 ± 0.06
spleen	0.45 ± 0.05	0.61 ± 0.10	0.39 ± 0.04	0.67 ± 0.04
liver	17.67 ± 3.42	25.64 ± 2.12	22.80 ± 1.84	17.41 ± 0.75
skin	3.96 ± 0.22	9.10 ± 0.61	3.18 ± 0.40	4.43 ± 0.27
brain	0.12 ± 0.00	0.098 ± 0.014	0.18 ± 0.01	0.069 ± 0.014
		Regional Brain Distribution (% dose/g) at 60 min Postinjection (Region/CB)[b]		
cerebellum	0.057 ± 0.003 (1.00)	0.038 ± 0.001 (1.00)	0.070 ± 0.002 (1.00)	0.039 ± 0.006 (1.00)
striatum	0.151 ± 0.002 (2.66)	0.083 ± 0.012 (2.18)	0.198 ± 0.013 (2.82)	0.046 ± 0.006 (1.17)
hippocampus	0.096 ± 0.015 (1.69)	0.067 ± 0.004 (1.76)	0.114 ± 0.003 (1.61)	0.039 ± 0.000 (1.00)
cortex	0.094 ± 0.012 (1.65)	0.052 ± 0.010 (1.37)	0.122 ± 0.014 (1.73)	0.051 ± 0.008 (1.30)

[a] Percentage dose/organ, average of three rats ± SD [b] Region/CB = percentage dose per gram of specific region/percentage dose per gram of cerebellum.

Table 3. Striatal/Cerebellar (ST/CB) Ratio in Rat Brain Post iv Injection of [^{99m}Tc]TRODAT-1, **13**[a]

	2 min	30 min	60 min	120 min	240 min	360 min
ST/CB ratio	0.93 ± 0.23	2.04 ± 0.18	2.66 ± 0.01	3.90 ± 1.33	4.07 ± 0.54	2.97 ± 0.14

[a] Striatal/cerebellar (ST/CB) ratio: percentage dose per gram of striatum/percentage dose per gram of cerebellum (average of three rats ± SD).

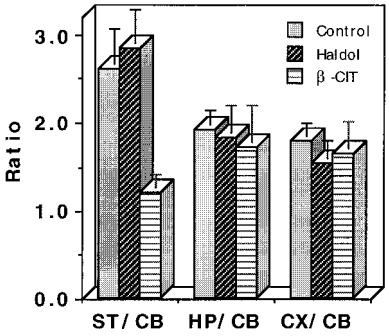

Figure 2. Ratios of regional brain uptakes at 60 min post iv injection of [^{99m}Tc]TRODAT-1 (**13**) in control rats and rats pretreated with haldol (1 mg/kg, iv) or β-CIT (1 mg/kg, iv) 5 min prior to radiotracer injection. Values shown are means ± SD (n = 3−4, p < 0.05, Student's t-test). ST, striatum; HP, hippocampus; CX, cortex; CB, cerebellum. The ST area, where dopamine transporters are located, displayed selective regional brain uptake, with the highest concentration ratio (ST/CB = 2.6). Pretreatment with β-CIT, which competes for dopamine transporter binding, showed blocking of specific uptake of [^{99m}Tc]TRODAT-1 (**13**) in the ST area.

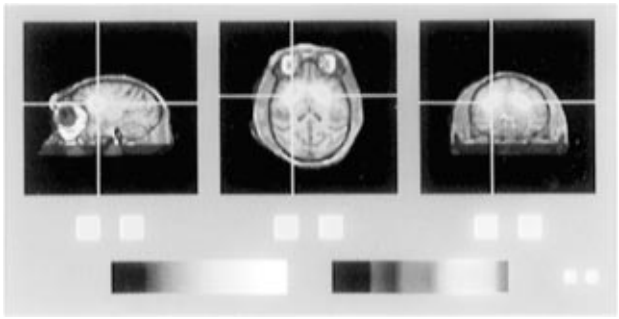

Figure 3. Transaxial, coronal, and sagittal SPECT images (1.34 mm thick) of baboon brain at 60−90 min post iv injection of 9 mCi of [^{99m}Tc]TRODAT-1 (**13**). SPECT images were acquired by a Picker T3000 scanner. The SPECT images were coregistered with the same sections of MRI of the same baboon. A high accumulation of [^{99m}Tc]TRODAT-1 (**13**) was observed in caudate and putamen, areas of the brain where dopamine transporters are concentrated.

in this paper strongly suggests that this compound may potentially be useful for studying dopamine transporters, there are a number of questions that remain unanswered. Correlation of dopamine transporter uptake as measured by SPECT imaging and the actual neuronal integrity requires extensive kinetic modeling studies to validate and estimate the potential clinical utility. Optimized imaging protocol and reproducibility of SPECT imaging of this new agent remain to be investigated.

Formation of ReO and TcO complexes with mono-N-substituted N_2S_2 ligands can lead to four isomers. Two enantiomers (*R* and *S*) are formed from the quaternary amine nitrogen and two sets of diastereomers (syn and anti) are formed by the orientation of the N-substituent in relation to the metal−oxygen bond. In general, the syn diastereomers are formed preferentially to the anti

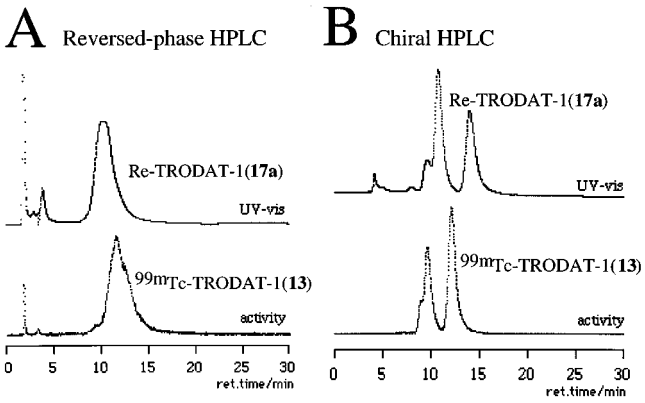

Figure 4. (A) Comparison of HPLC profiles of [^{99m}Tc]TRODAT-1 (**13**; lower profile, radioactivity trace) and Re-TRODAT-1 (**17a**; upper profile, UV−vis 254 nm) coinjected onto a reversed-phase column (PRP-1) with acetonitrile:DMGA buffer (pH 7) in a ratio of 80:20 and a flow rate of 1 mL/min. (B) Comparison of HPLC profiles of [^{99m}Tc]TRODAT-1 (**13**; lower profile, radioactivity trace) and Re-TRODAT-1 (**17a**; upper profile, UV−vis 254 nm) coinjected onto a Chiralpak AD (chiral) column with hexane:EtOH in a ratio of 3:1 and a flow rate of 1 mL/min. Generally, the retention times of Re complexes are comparable to those of Tc-99m compounds.

diastereomers. The formation of predominantly syn diastereomers of TcO complexes with mono-N-substituted N_2S_2 ligands has been documented previously by several research groups.[27,36−38] Since the N_2S_2 ligands **12a**−**c** carry a N-substitution group with an additional chiral center (tropanyl moiety), all of the possible metal−oxo complexes become diastereomers. However, HPLC analyses of the crude reaction mixtures of the [^{99m}Tc]TRODAT complexes (**13**) indicated the presence of two major isomers in a ratio of about 1:0.8. Although these isomers displayed similar elution profiles on reversed-phase HPLC, they have different retention times on HPLC profiles obtained using a chiral column (Figure 4). Similarly, the corresponding ReO complexes **17a**,**b** also contained two major isomers, as evidenced by TLC, ^{1}H NMR, and HPLC (Figure 4), and they have comparable retention times to the Tc-99m-oxo-TRODAT complexes (**13**). To further resolve the structures of the individual isomers, we are in the process of obtaining suitable crystals of each rhenium isomer to be used for X-ray structure determination.

Conclusion

A novel series of Tc-99m-labeled complexes was reported. One of the compounds, [^{99m}Tc]TRODAT-1 (**13**), may potentially be useful for *in vivo* measurement of dopamine neuronal loss related to changes in dopamine transporters.[39,40]

Experimental Section

General. Reagents used in the syntheses were purchased from Aldrich (Milwaukee, WI) or Fluka (Ronkonkoma, NY) and used without further purification unless otherwise indicated. Anhydrous Na_2SO_4 was used as a drying agent. Reaction yields are reported without attempts at optimization. Thin layer chromatography was performed on EM Science (Gibbstown, NJ) precoated (0.2 mm) silica gel 60 plates, and the spots were detected with iodine vapor and/or UV light. Silica gel 60 (70−230 mesh), obtained from EM Science (Gibbstown, NJ), was used for column chromatography. ^{1}H NMR spectra were obtained on a Bruker spectrometer (Bruker AC 300). All samples prepared for NMR analysis were dissolved in $CDCl_3$, purchased from Aldrich. Chemical shifts are reported as δ values with chloroform or TMS as the internal reference. Coupling constants are reported in hertz (Hz). The multiplicity is defined by s (singlet), d (doublet), t (triplet), brs (broad signal), dt (doublet of triplet), and m (multiplet). IR spectra were recorded with a Mattson Polaris FT-IR spectrometer and are reported in cm^{-1}. Melting points were determined on a Meltemp apparatus (Cambridge, MA) and are uncorrected. Elemental analyses were performed by Atlantic Microlabs (Norcross, GA). High-resolution mass spectrometry was performed by the Nebraska Center for Mass Spectroscopy, University of Nebraska, Lincoln, NE. Compounds **1**−**4** were synthesized according to the literature.[9,34] $[Bu_4N][ReOCl_4]$ was prepared according to the literature method.[41]

Preparation of Compounds 6a−c. Oxalyl chloride (2 mmol, 1 mL from 2 M solution in CH_2Cl_2) was added to tropane acid **4** (1 mmol) in CH_2Cl_2 (10 mL) at room temperature under N_2. The resulting mixture was stirred for 1.5 h and concentrated *in vacuo* at 30 °C to obtain a viscous oil, which was dried in a vacuum for 15 min. The acid chloride obtained was dissolved in CH_2Cl_2 (10 mL) and cooled to −10 °C, and amine **2** (1 mmol, 197 mg) in CH_2Cl_2 (10 mL) was added followed by Et_3N (2 mmol, 0.28 mL) under N_2. The resulting solution was stirred at room temperature for 6 h. Water (20 mL) was then added to the reaction mixture, and the product was extracted into CH_2Cl_2 (3 × 20 mL). The CH_2Cl_2 layers were combined, dried over Na_2SO_4, and concentrated *in vacuo* to produce an oil that was chromatographed on silica gel (EtOAc:MeOH:NH_4-OH, 8.5:1:0.5) to obtain the title compound as a viscous oil.

3-(4-Chlorophenyl)-*N*-[2-[*S*-(4-methoxybenzyl)thio]ethyl]-8-azabicyclo[3.2.1]octane-2-carboxamide-[1*R*-(*exo-exo*)] (6a): yield 63%; IR ($CHCl_3$) 1656 cm^{-1}; ^{1}H NMR ($CDCl_3$) δ 1.55−1.78 (m, 3H), 2.05−2.6 (m, 9H), 3.1−3.4 (m, 5H), 3.69 (s, 2H), 3.79 (s, 3H), 6.84 (d, 2H, J = 6 Hz), 7.09 (d, 2H, J = 6 Hz), 7.18 (d, 2H, J = 6 Hz), 7.24 (d, 2H, J = 6 Hz), 9.8 (brs, 1H); HRMS *m/z* 458.1794 calculated for $C_{25}H_{31}O_2N_2SCl$, M^+ + 1, 459.1994.

3-(4-Fluorophenyl)-*N*-[2-[S-(4-methoxybenzyl)thio]ethyl]-8-azabicyclo[3.2.1]octane-2-carboxamide-[1*R*-(*exo-exo*)] (6b): yield 59%; IR ($CHCl_3$) 1653 cm^{-1}; ^{1}H NMR ($CDCl_3$) δ 1.59−1.76 (m, 3H), 1.97−2.4 (m, 6H), 2.4−2.5 (m, 3H), 3.09 (m, 1H), 3.3−3.38 (m, 4H), 3.68 (s, 2H), 3.78 (s, 3H), 6.8−6.9 (m, 4H), 7.08−7.13 (m, 2H), 7.2 (d, 2H, J = 10 Hz), 9.8 (brs, 1H); HRMS *m/z* 442.2090 calculated for $C_{25}H_{31}O_2N_2SF$, M^+ + 1, 443.2161.

3-(4-Bromophenyl)-*N*-[2-[*S*-(4-methoxybenzyl)thio]ethyl]-8-azabicyclo[3.2.1]octane-2-carboxamide-[1*R*-(*exo-exo*)] (6c): yield 53%; IR ($CHCl_3$) 1651 cm^{-1}; ^{1}H NMR ($CDCl_3$) δ 1.53−1.78 (m, 3H), 1.93−2.5 (m, 6H), 2.6−2.7 (m, 3H), 3.05 (m, 1H), 3.2−3.38 (m, 4H), 3.64 (s, 2H), 3.78 (s, 3H), 6.84 (d, 2H, J = 8.7 Hz), 7.03 (d, 2H, J = 8.4 Hz), 7.23 (d, 2H, J = 8.7 Hz), 7.32 (d, 2H, J = 8.4 Hz), 9.8 (brs, 1H); HRMS *m/z* 502.1289 calculated for $C_{25}H_{31}O_2N_2SBr$, M^+ + 1, 503.1164.

Preparation of Compounds 8a−c. BH_3·THF (5 mmol, 5 mL of 1 M solution in THF) was added to compounds **6a**−**c** (1 mmol) in THF (10 mL) under N_2, and the resulting mixture was heated at reflux for 12 h. The reaction mixture was cooled to 0 °C, and 1 N HCl was added dropwise until no more gas evolution was observed; then the mixture was concentrated *in vacuo*. HCl (1 N, 10 mL) was added to the viscous oil obtained, and the resulting mixture was stirred at 90 °C for 30 min. The solution was then cooled to 0 °C and basified with concentrated NH_4OH. The product was extracted into CH_2Cl_2 and purified by chromatography on silica gel (EtOAc: MeOH:NH_4OH, 8.5:1:0.5) to produce the title compound.

3-(4-Chlorophenyl)-2-[[*N*-[2-[*S*-(4-methoxybenzyl)thio]-ethyl]amino]methyl]-8-azabicyclo[3.2.1]octane-[1*R*-(*exo-exo*)] (8a): yield 79%; IR ($CHCl_3$) 1608 cm^{-1}; ^{1}H NMR ($CDCl_3$) δ 1.5−1.8 (m, 5H), 2.05−2.2 (m, 4H), 2.23 (s, 3H), 2.34−2.39 (m, 2H), 2.47−2.52 (m, 2H), 2.65 (dd, 1H, J_1 = 5.3 Hz, J_2 = 7.8 Hz), 3.03 (td, 1H, J_1 = 4 Hz, J_2 = 8.8 Hz), 3.25 (m, 2H), 3.5 (s, 2H), 3.78 (s, 3H), 6.84 (d, 2H, J = 6 Hz), 7.09 (d, 2H, J = 6 Hz), 7.18 (d, 2H, J = 6 Hz), 7.24 (d, 2H, J = 6 Hz); HRMS *m/z* 444.2002 calculated for $C_{25}H_{33}ON_2SCl$, M^+ + 1, 444.1963.

**3-(4-Fluorophenyl)-2-[[*N*-[2-[*S*-(4-methoxybenzyl)thio]-ethyl]amino]methyl]-8-azabicyclo[3.2.1]octane-[1*R*-(*exo-*

***exo*)] (8b):** yield 83%; IR ($CHCl_3$) 1600 cm^{-1}; ^1H NMR ($CDCl_3$) δ 1.59−1.76 (m, 5H), 2.0−2.8 (m, 12H), 3.09 (m, 1H), 3.2−3.38 (m, 2H), 3.68 (s, 2H), 3.78 (s, 3H), 6.8−6.9 (m, 4H), 7.08−7.13 (m, 2H), 7.2 (d, 2H, J = 10 Hz); HRMS *m/z* 428.2297 calculated for $C_{25}H_{33}ON_2SF$, $M^+ + 1$, 429.1543.

3-(4-Bromophenyl)-2-[[*N*-[2-[*S*-(4-methoxybenzyl)thio]ethyl]amino]methyl]-8-azabicyclo[3.2.1]octane-[1*R*-(*exo*-*exo*)] (8c): yield 77%; IR ($CHCl_3$) 1600 cm^{-1}; ^1H NMR ($CDCl_3$) δ 1.59−1.76 (m, 5H), 2.0−2.8 (m, 12H), 3.03 (m, 1H), 3.2−3.42 (m, 2H), 3.7 (s, 2H), 3.78 (s, 3H), 6.84 (d, 2H, J = 8.7 Hz), 7.00 (d, 2H, J = 8.4 Hz), 7.21 (d, 2H, J = 8.7 Hz), 7.22 (d, 2H, J = 8.4 Hz); HRMS *m/z* 488.1496 calculated for $C_{25}H_{33}ON_2SBr$, $M^+ + 1$, 489.1543.

Preparation of Compounds 9a-c. Amine **2** (12.5 mmol, 2.46 g) in CH_2Cl_2 (15 mL) was added dropwise to a stirred solution of chloroacetyl chloride (12.5 mmol, 1 mL) in CH_2Cl_2 (15 mL) followed by Et_3N (12.5 mmol, 1.7 mL) at −78 °C under N_2. The reaction mixture was allowed to warm to room temperature and stirred for 1 h. Water (20 mL) was then added, and the organic layer was separated and washed with 1 N HCl (20 mL), brine (20 mL), and water (20 mL). The organic layer was concentrated *in vacuo* and dried *in vacuo* for 30 min. The oil was dissolved in EtOAc (50 mL) and hexane (100 mL). The turbid solution obtained was concentrated to one-half the volume and stored in a freezer for 4 h. The solid formed was collected by suction filtration to produce compound **7**, which was used for further reactions without additional purification.

Amines **8a**−**c** (1 mmol), chloro compound **7** (2 mmol, 548 mg), and Et_3N (2 mmol, 0.28 mL) in acetonitrile (10 mL) were heated at reflux for 12 h. The reaction mixture was concentrated *in vacuo*, and the product was partitioned between water (20 mL) and CH_2Cl_2 (20 mL). The oil obtained by concentrating the organic phase was chromatographed on silica gel. An impurity was washed out with MeOH:CH_2Cl_2 (1:9). The title compound was eluted with MeOH:CH_2Cl_2 (2:8) and isolated as a yellow oil.

2-[[[3-(4-Chlorophenyl)-8-methyl-8-azabicyclo[3.2.1]-oct-2-yl]methyl][2-[*S*-(4-methoxybenzyl)thio]ethyl]amino]-*N*-[2-[*S*-(4-methoxybenzyl)thio)ethyl]actamide-[1*R*-(*exo*-*exo*)] (9a): yield 53%; IR ($CHCl_3$) 1654 cm^{-1}; ^1H NMR ($CDCl_3$) δ 1.4−1.8 (m, 5H), 2.05−2.9 (m, 13H), 2.92−3.5 (m, 7H), 3.52 (s, 2H), 3.95 (s, 2H), 3.76 (s, 6H), 6.8−6.85 (m, 4H), 6.9 (d, 2H, J = 6 Hz), 7.15−7.25 (m, 6H), 8.4 (brs, 1H); HRMS *m/z* 681.2825 calculated for $C_{37}H_{48}O_3N_3S_2Cl$, $M^+ + 1$, 682.2927.

2-[[[3-(4-Fluorophenyl)-8-methyl-8-azabicyclo[3.2.1]-oct-2-yl]methyl][2-[*S*-(4-methoxybenzyl)thio]ethyl]amino]-*N*-[2-[*S*-(4-methoxybenzyl)thio]ethyl]actamide-[1*R*-(*exo*-*exo*)] (9b): yield 66%; IR ($CHCl_3$) 1650 cm^{-1}; ^1H NMR ($CDCl_3$) δ 1.34−1.72 (m, 5H), 2.0−2.77 (m, 13H), 2.82−3.48 (m, 7H), 3.53 (s, 2H), 3.66 (s, 2H), 3.71 (s, 6H), 6.79−6.85 (m, 4H), 6.9−7.03 (m, 2H), 7.18−7.45 (m, 6H), 8.4 (brs, 1H); HRMS *m/z* 665.3121 calculated for $C_{37}H_{48}O_3N_3S_2F$, $M^+ + 1$, 666.2927.

2-[[[3-(4-Bromophenyl)-8-methyl-8-azabicyclo[3.2.1]oct-2-yl]methyl][2-[*S*-(4-methoxybenzyl)thio]ethyl]amino]-*N*-[2-[*S*-(4-methoxybenzyl)thio]ethyl]actamide-[1*R*-(*exo*-*exo*)] (9c): yield 56%; IR ($CHCl_3$) 1648 cm^{-1}; ^1H NMR ($CDCl_3$) δ 1.38−1.76 (m, 5H), 2.0−2.81 (m, 13H), 2.88−3.46 (m, 7H), 3.58 (s, 2H), 3.68 (s, 2H), 3.77 (s, 6H), 6.76−6.82 (m, 4H), 6.93 (d, 2H, J = 8.7 Hz), 7.13−7.21 (m, 4H), 7.34 (d, 2H, J = 8.7 Hz), 8.4 (brs, 1H); HRMS *m/z* 725.2320 calculated for $C_{37}H_{48}O_3N_3S_2Br$, $M^+ + 1$, 726.2110.

Preparation of Compounds 11a−c. BH_3·THF (1.5 equiv) was added to a solution of compounds **9a**−**c** (1 mmol) in THF (10 mL) under N_2, and the resulting mixture was heated at reflux for 12 h. Workup of this reaction mixture was carried out as described for compounds **8a**−**c** followed by chromatography of the resulting product on a chromatotron (EtOAc:MeOH:NH_4OH, 8.5:1:0.5), producing the title compound.

2-[[2-[[[3-(4-Chlorophenyl)-8-methyl-8-azabicyclo[3.2.1]-oct-2-yl]methyl][[*S*-(4-methoxybenzyl)thio]ethyl]amino]-*S*-(4-methoxybenzyl)ethanethiol (11a): yield 71%; IR ($CHCl_3$) 1609 cm^{-1}; ^1H NMR ($CDCl_3$) δ 1.5−1.8 (m, 5H), 2.05−2.3 (m, 5H), 2.3 (s, 3H), 2.3−2.6 (m, 7H), 2.7−2.9 (m, 5H), 3.1 (td, 1H, J_1 = 4 Hz, J_2 = 8.8 Hz), 3.35−3.45 (m, 2H), 3.59 (s, 2H), 3.65−3.7 (m, 2H), 3.76 (s, 6H), 6.8−6.85 (m, 4H), 7.15−7.25 (m, 8H); HRMS *m/z* 667.3032 calculated for $C_{37}H_{50}O_2N_3S_2Cl$, $M^+ + 1$, 668.3115.

2-[[2-[[[3-(4-Fluorophenyl)-8-methyl-8-azabicyclo[3.2.1]-oct-2-yl]methyl][[*S*-(4-methoxybenzyl)thio]ethyl]amino]-*S*-(4-methoxybenzyl)ethanethiol (11b): yield 63%; IR ($CHCl_3$) 1603 cm^{-1}; ^1H NMR ($CDCl_3$) δ 1.4−1.7 (m, 5H), 1.95−2.29 (m, 5H), 2.25−2 (m, 10H), 2.7−2.9 (m, 5H), 3.0 (td, 1H, J_1 = 4 Hz, J_2 = 8.8 Hz), 3.2 (m, 1H), 3.35 (m, 1H), 3.6 and 3.65 (s, 2H each), 3.7 and 3.77 (s, 3H each), 6.7−6.8 (m, 4H), 6.9−6.96 and 7.01−7.06 (m, 2H each), 7.16−7.22 (m, 4H); HRMS *m/z* 651.3328 calculated for $C_{37}H_{50}O_2N_3S_2F$, $M^+ + 1$, 652.3145.

2-[[2-[[[3-(4-Bromophenyl)-8-methyl-8-azabicyclo[3.2.1]-oct-2-yl]methyl][[*S*-(4-methoxybenzyl)thio]ethyl]amino]-*S*-(4-methoxybenzyl)ethanethiol (11c): yield 68%; IR ($CHCl_3$) 1603 cm^{-1}; ^1H NMR ($CDCl_3$) δ 1.4−1.7 (m, 5H), 1.95−2.29 (m, 5H), 2.25−2 (m, 10H), 2.7−2.9 (m, 5H), 3.0 (td, 1H, J_1 = 4 Hz, J_2 = 8.8 Hz), 3.2 (m, 1H), 3.35 (m, 1H), 3.6 and 3.65 (s, 2H each), 3.7 and 3.77 (s, 3H each), 6.7−6.8 (m, 4H), 6.93 (d, 2H, J = 8.4 Hz), 7.15−7.25 (m, 4H), 7.3 (d, 2H, J = 9.1 Hz); HRMS *m/z* 711.2528 calculated for $C_{37}H_{50}O_2N_3S_2Br$, $M^+ + 1$, 712.2626.

General Procedure for Compounds 10 and 12a−c. Substrate **9a** or **11a**−**c** (1 mmol) was dissolved in TFA (7.5 mL) and anisole (0.25 mL) at 0 °C, and $Hg(OAc)_2$ (636 mg, 2 mmol) was added. The resulting mixture was stirred for 30 min and concentrated *in vacuo* to obtain a viscous oil that was dried *in vacuo* for 30 min. Dry ether (10 mL) was then added to the above oil, and the resulting suspension was sonicated for 5 min. The colorless solid that formed was collected by suction filtration, dried *in vacuo* for 20 min, and dissolved in absolute EtOH (10 mL). H_2S gas was passed through the solution for 20 min, and the reaction mixture was filtered through a pad of Celite. The filtrate was concentrated *in vacuo* to obtain the trifluoroacetate salts of the title compounds, which were used for further reactions without additional purification.

Preparation of Compounds 17a,b. A solution of compound **12a** or **12b** (1 mmol) in MeOH (10 mL) was added to a solution of $[Bu_4N][ReOCl_4]$[41] (588 mg, 1 mmol) in MeOH (2 mL) under N_2 at 0 °C. Et_3N (0.5 mL, 4 mmol) was then added, and the resulting mixture was stirred at room temperature for 12 h. The reaction mixture was concentrated *in vacuo*. The residue obtained was chromatographed on silica gel (EtOAc:MeOH:NH_4OH, 9.5:0.4:0.1) to obtain a purple solid, which was recrystallized (MeOH:CH_2Cl_2) to give pinkish needles.

2*β*-{Oxo[*N*,*N*′-bis(2-mercaptoethyl)ethylenediaminato]-rhenium(V)methyl}-3*β*-(4-chlorophenyl)tropane (17a): yield 43%; IR (KBr) 933 cm^{-1}; HRMS *m/z* 627.1154, calculated for $C_{21}H_{31}ON_3S_2ClRe$, $M^+ + 1$, 628.1249.

2*β*-{Oxo[*N*,*N*′-bis(2-mercaptoethyl)ethylenediaminato]-rhenium(V)methyl}-3*β*-(4-fluorophenyl)tropane (17b): yield 49%; IR (KBr) 938 cm^{-1}; HRMS *m/z* 611.1450, calculated for $C_{21}H_{31}ON_3S_2FRe$, $M^+ + 1$, 612.1569.

Radiolabeling with Tc-99m. The appropriate ligand (**12a**−**c** or **10**; 0.2−0.4 μmol) was dissolved in 100 μL of EtOH and 100 μL of HCl (1 N). HCl (500 μL, 1 N), 1 mL of Sn-glucoheptonate solution (containing 136 μg of $SnCl_2$ and 200 μg of Na-glucoheptonate, pH 6.67), and 50 μL of EDTA solution (0.1 N) were successively added. [^{99m}Tc]Pertechnetate (100−200 μL, range of 1−20 mCi) in saline solution was then added. The reaction mixture was heated for 30 min at 100 °C (or heated at 125 °C in an autoclave for 30 min), cooled to room temperature, and neutralized with a saturated $NaHCO_3$ solution. After the complex was extracted from the aqueous reaction medium with ethyl acetate (1 × 3 mL, 2 × 1.5 mL) and passed through a small column of Na_2SO_4, ethyl acetate was removed under a flow of N_2. The residue was dissolved in 200 μL of EtOH and purified by HPLC (PRP-1 column, 250 × 4.1 mm, CH_3CN/3,3-dimethylglutarate buffer, 5 mM, pH 7, volume ratio 8:2, flow rate 1 mL/min). The retention times for the stereoisomers of **13** were 10.5 and 11.5 min (radiochemical yield 88%, radiochemical purity >98%). All of the complexes displayed *in vitro* stability at 4 and 24 h after preparation. Little change in radiochemical purity was observed. Identical labeling and HPLC conditions were used for

the preparation of mixtures of **14**−**16** (retention times of 9.4 and 10.1, 14.2 and 15.6, and 7.8 and 8.9 min, respectively) with radiochemical yields of 70%, 88%, and 80%, respectively, and radiochemical purities of >98%.

Partition Coefficients. Partition coefficients were measured by mixing each Tc-99m compound with 3 g each of 1-octanol and buffer (pH 7.0, 0.1 M phosphate) in a test tube. The test tube was vortexed for 3 min at room temperature and then centrifuged for 5 min. Two weighted samples (0.5 g each) from the 1-octanol and buffer layers were counted in a well counter. The partition coefficient was determined by calculating the ratio of cpm/g of 1-octanol to that of buffer. Samples from the 1-octanol layer were repartitioned until consistent partition coefficient values were obtained. The measurement was repeated three times.

Biodistribution in Rats. Male Sprague−Dawley rats (225−300 g), allowed free access to food and water, were used for *in vivo* biodistribution studies.[42,43] While under ether anesthesia, 0.2 mL of a saline solution containing **13**, **14**, **15**, or **16** (50−100 μCi) was injected directly into the femoral vein of rats, and the rats were sacrificed by cardiac excision at various time points postinjection. The organs of interest were removed and weighed, and the radioactivity was counted with an automatic gamma counter (Packard 5000). The percentage dose per organ was calculated by a comparison of the tissue counts to suitably diluted aliquots of the injected material. Total activities of blood and muscle were calculated under the assumption that they were 7% and 40% of the total body weight, respectively.

Regional brain distribution in rats was obtained after an injection of **13**, **14**, **15**, or **16**. Samples from different brain regions (cortex, striatum, hippocampus, and cerebellum) were dissected, weighed, and counted, and the percentage dose per gram of sample was calculated by comparing the sample counts with the count of the diluted initial dose. The uptake ratio of each region was obtained by dividing the percentage dose per gram of that region by that of the cerebellum. For blocking studies, rats were injected with either β-CIT or haloperidol (iv, 1 mg/kg) 5 min prior to the injection of **13**. The rats were dissected, and brain tissue samples were counted as described above. The specific uptake of the compound was expressed as a ratio of ST/CB (percentage dose/g of striatum divided by percentage dose/g of cerebellum).

SPECT and MRI Imaging in a Baboon. A baboon (~15 kg) was the subject of a SPECT imaging study. Prior to imaging, the animal was fasted, immobilized with ketamine (10−20 mg/kg, im) and xylazine (2−3 mg/kg, im), intubated, and maintained on an 1.5−2.0% isofluorane/98.5% oxygen mixture (flow rate of 200−500 cc/min). The animal was injected with glycopyrrolate (10 μg/kg, sc), an anticholinergic drug that does not cross the blood−brain barrier, in order to decrease digestive and respiratory secretions. Body temperature was maintained using a hot water-circulating heating pad and monitored with a rectal thermometer. The animal's head was immobilized using a vacuum-packed bean-bag device that hardens upon evacuation when molded around the head. No-carrier-added [^{99m}Tc]TRODAT-1 (**13**; 9 mCi) was administered as an iv bolus in the saphenous vein of the baboon. Immediately after injection, sequential 5 min/frame dynamic SPECT scans were acquired on a triple-headed Picker Prism 3000 camera (fwhm: 7 mm) equipped with fan beam collimators for 2 h. The acquisition parameters were a 20% energy window at 140 keV, 120 projection angles over 360°, a 128 × 128 matrix, and a zoom factor of 1.78 in a slice thickness of 2 mm cubic voxels. The projection data were reconstructed with a count-dependent 3-D Wiener filter. Chang's first-order correction method was used to compensate for attenuation. Magnetic resonance images (MRI) of the baboon brain were acquired with a 1.5 T machine (GE Medical Systems, Milwaukee, WI). The spoiled GRASS acquisition parameters for T_1 weighted images included a repetition time (TR) of 5 ms and a flip angle of 35°, which produced 1 mm thick slices. The data were reinterpolated in 256 × 256 matrices with cubic voxels of 2 mm/side to match the SPECT images. The SPECT images of [^{99m}Tc]TRODAT-1 (**13**) at 60−90 min postinjection were summed and reformatted to coregister with the MRI scans of the same baboon. The coregistration program simultaneously displayed three orthogonal views of either the MRI or the SPECT scans (coronal, transaxial, and sagittal views). When alignment was achieved, images of SPECT and MRI were displayed.

Acknowledgment. This work was supported by grants awarded by the National Institutes of Health (H.F.K.; NS24538 and NS18509) and the Department of Energy (H.F.K.; ER61657). The authors thank Ms. Susan West for her editorial assistance.

References

(1) Carroll, F. I.; Scheffel, U.; Dannals, R. F.; Boja, J. W.; Kuhar, M. J. Development of imaging agents for the dopamine transporter. *Med. Res. Rev.* **1995**, *15*, 419−444.

(2) Carroll, F. I.; Mascarella, S. W.; Kuzemko, M. A.; Gao, Y.; Abraham, P.; Lewin, A. H.; Boja, J. W.; Kuhar, M. J. Synthesis, ligand binding, and QSAR (CoMFA and classical) study of 3β-(3′-substituted phenyl)-, 3β-(4′-substituted phenyl)-, and 3β-(3′,4′-disubstituted phenyl)tropane-2β-carboxylic acid methyl esters. *J. Med. Chem.* **1994**, *37*, 2865−2873.

(3) Carroll, F. I.; Kotian, P.; Dehghani, A.; Gray, J. L.; Kuzemko, M. A.; Parham, K. A.; Abraham, P.; Lewin, A. H.; Boja, J. W.; Kuhar, M. J. Cocaine and 3β-(4′-substituted phenyl)tropane-2β-carboxylic acid ester and amide analogues. New high-affinity and selective compounds for the dopamine transporter. *J. Med. Chem.* **1995**, *38*, 379−388.

(4) Volkow, N. D.; Fowler, J. S.; Gatley, S. J.; Logan, J.; Wang, G.-J.; Ding, Y.-S.; Dewey, S. PET evaluation of the dopamine system of the human brain. *J. Nucl. Med.* **1996**, *37*, 1242−1253.

(5) Yu, D.-W.; Gatley, S. J.; Wolf, A. P.; MacGregor, R. R.; Dewey, S. L.; Fowler, J. S.; Schlyer, D. J. Synthesis of carbon-11-labeled iodinated cocaine derivatives and their distribution in baboon brain measured using positron emission tomography. *J. Med. Chem.* **1992**, *35*, 2178−2183.

(6) Fowler, J. S.; Volkow, N. D.; MacGregor, R. R.; Logan, J.; Dewey, S. L.; Gatley, S. J.; Wolf, A. P. Comparative PET studies of the kinetics and distribution of cocaine and cocaethylene in baboon brain. *Synapse* **1992**, *12*, 220−227.

(7) Frost, J. J.; Rosier, A. J.; Reich, S. G.; Smith, J. S.; Ehlers, M. D.; Snyder, S. H.; Ravert, H. T.; Dannals, R. F. Positron emission tomographic imaging of the dopamine transporter with [^{11}C]-WIN 35,428 reveals marked declines in mild Parkinson's disease. *Ann. Neurol.* **1993**, *34*, 423−431.

(8) Wong, D. F.; Yung, B.; Dannals, R. F.; Shaya, E. K.; Ravert, H. T.; Chen, C. A.; Chan, B.; Folio, T.; Scheffel, U.; Ricaurte, G. A.; Neumeyer, J. L.; Wagner, H. N., Jr.; Kuhar, M. J. *In vivo* imaging of baboon and human dopamine transporters by positron emission tomography using [^{11}C]WIN35,428. *Synapse* **1993**, *15*, 130−142.

(9) Meltzer, P. C.; Liang, A. Y.; Brownell, A.-L.; Elmaleh, D. R.; Madras, B. K. Substituted 3-phenyltropane analogs of cocaine: synthesis, inhibition of binding at cocaine recognition sites, and positron emission tomography imaging. *J. Med. Chem.* **1993**, *36*, 855−862.

(10) Innis, R. B.; Seibyl, J. P.; Scanley, B. E.; Laruelle, M.; Abi-Dargham, A.; Wallace, E.; Baldwin, R. M.; Zea-Ponce, Y.; Zoghbi, S.; Wang, S.; et al. Single photon emission computed tomographic imaging demonstrates loss of striatal dopamine transporters in Parkinson's disease. *Proc. Natl. Acad. Sci. U.S.A.* **1993**, *90*, 11965−11969.

(11) Seibyl, J. P.; Laruelle, M. A.; Van Dyck, C. H.; Wallace, E.; Baldwin, R. M.; Zoghbi, S. S.; Zea-Ponce, Y.; Neumeyer, J. L.; Charney, D. S.; Hoffer, P. B.; Innis, R. B. Reproducibility of iodine-123-β-CIT SPECT brain measurement of dopamine transporters. *J. Nucl. Med.* **1996**, *37*, 222−228.

(12) Kuikka, J. T.; Akerman, K.; Bergstrom, K. A.; Karhu, J.; Hiltunen, J.; Haukka, J.; Heikkinen, J.; Tiihonen, J.; Wang, S.; Neumeyer, J. L. Iodine-123-labeled N-(2-fluoroethyl)-2β-carbomethoxy-3β-(4-iodophenyl)nortropane for dopamine transporter imaging in the living human brain. *Eur. J. Nucl. Med.* **1995**, *22*, 682−686.

(13) Neumeyer, J. L.; Wang, S.; Gao, Y.; Milius, R. A.; Kula, N. S.; Campbell, A.; Baldessarini, R. J.; Zea-Ponce, Y.; Baldwin, R. M.; Innis, R. B. N-ω-Fluoroalkyl analogs of (1*R*)-2β-carbomethoxy-3β-(4-iodophenyl)-tropane (β-CIT): radiotracers for positron emission tomography and single photon emission computed tomography imaging of dopamine transporters. *J. Med. Chem.* **1994**, *37*, 1558−1561.

(14) Mozley, P. D.; Stubbs, J. B.; Kim, H.-J.; McElgin, W.; Kung, M.-P.; Meegalla, S.; Kung, H. F. Dosimetry of an iodine-123-labeled tropane to image dopamine transporters. *J. Nucl. Med.* **1996**, *37*, 151−159.

(15) Abi-Dargham, A.; Gandelman, M. S.; DeErausquin, G. A.; Zea-Ponce, Y.; Zoghbi, S. S.; Baldwin, R. M.; Laruelle, M.; Charney, D. S.; Hoffer, P. B.; Neumeyer, J. L.; Innis, R. B. SPECT imaging of dopamine transporters in human brain with iodine-123-fluoroalkyl analogs of β-CIT. *J. Nucl. Med.* **1996**, *37*, 1129−1133.
(16) Kilbourn, M. R. *In vivo* binding of [^{18}F]GBR13119 to the brain dopamine uptake system. *Life Sci.* **1988**, *42*, 1347−1353.
(17) Innis, R. B. Single photon emission tomography imaging of dopamine terminal innervation: a potential clinical tool in Parkinson's disease [editorial; review]. *Eur. J. Nucl. Med.* **1994**, *21*, 1−5.
(18) Goodman, M. M.; Kung, M.-P.; Kabalka, G. W.; Kung, H. F.; Switzer, R. Synthesis and characterization of radioiodinated N-(3-iodopropen-1-yl)-2β-carbomethoxy-3β-(4-chlorophenyl)tropanes: potential dopamine reuptake site imaging agents. *J. Med. Chem.* **1994**, *37*, 1535−1542.
(19) Malison, R. T.; Vessotskie, J. M.; Kung, M.-P.; McElgin, W.; Romaniello, G.; Kim, H.-J.; Goodman, M. M.; Kung, H. F. Striatal dopamine transporter imaging in nonhuman primates with iodine-123-IPT SPECT. *J. Nucl. Med.* **1995**, *36*, 2290−2297.
(20) Kung, M.-P.; Essman, W. D.; Frederick, D.; Meegalla, S.; Goodman, M.; Mu, M.; Lucki, I.; Kung, H. F. IPT: a novel iodinated ligand for the CNS dopamine transporter. *Synapse* **1995**, *20*, 316−324.
(21) Jurisson, S. S.; Berning, D.; Jia, W.; Ma, D.-S. Coordination compounds in nuclear medicine. *Chem. Rev.* **1993**, *93*, 1137−1156.
(22) Steigman, J.; Eckelman, W. C. *The Chemistry of Technetium In Medicine*;. National Academy: Washington, DC, 1992.
(23) Lever, S. Z.; Baidoo, K. E.; Mahmood, A.; Matsumura, K.; Scheffel, U. A.; Wagner, H. N., Jr. Novel technetium ligands with affinity for the muscarinic cholinergic receptor. *Nucl. Med. Biol.* **1994**, *21*, 157−164.
(24) Del Rosario, R. B.; Jung, Y.-W.; Baidoo, K. E.; Lever, S. Z.; Wieland, D. M. Synthesis and *in vivo* evaluation of a [$^{99m/99}$Tc]-DADT-benzovesamicol: a potential marker for cholinergic neurons. *Nucl. Med. Biol.* **1994**, *21*, 197−203.
(25) Chi, D. Y.; O'Neil, J. P.; Anderson, C. J.; Welch, M. J.; Katzenellenbogen, J. A. Homodimeric and heterodimeric bis(aminothiol) oxometal complexes with rhenium(V) and technetium(V). Control of heterodimeric complex formation and an approach to metal complexes that mimic steroid hormones. *J. Med. Chem.* **1994**, *37*, 928−937.
(26) Chi, D. Y.; Katzenellenbogen, J. A. Selective formation of heterodimeric bis-bidentate aminothiol-oxometal complexes of rhenium(V). *J. Am. Chem. Soc.* **1993**, *115*, 7045−7046.
(27) DiZio, J. P.; Fiaschi, R.; Davison, A.; Jones, A. G.; Katzenellenbogen, J. A. Progestin-rhenium complexes: metal-labeled steroids with high receptor binding affinity, potential receptor-directed agents for diagnostic imaging or therapy. *Bioconjugate Chem.* **1991**, *2*, 353−366.
(28) DiZio, J. P.; Anderson, C. J.; Davison, A.; Ehrhardt, G. J.; Carlson, K. E.; Welch, M. J.; Katzenellenbogen, J. A. Technetium- and rhenium-labeled progestins: synthesis, receptor binding and *in vivo* distribution of an 11-β-substituted progestin labeled with technetium-99 and rhenium-186. *J. Nucl. Med.* **1992**, *33*, 558−569.
(29) O'Neil, J. P.; Carlson, K. E.; Anderson, C. J.; Welch, M. J.; Katzenellenbogen, J. A. Progestin radiopharmaceuticals labeled with technetium and rhenium: synthesis, binding affinity, and *in vivo* distribution of a new progestin N_2S_2-metal conjugate. *Bioconjugate Chem.* **1994**, *5*, 182−193.
(30) O'Neil, J. P.; Wilson, S. R.; Katzenellenbogen, J. A. Preparation and structural characterization of monoamine-monoamide bis-(thiol) oxo complexes of technetium(V) and rhenium(V). *Inorg. Chem.* **1994**, *33*, 319−323.
(31) Jurisson, S. S.; Pirro, J.; Di Rocco, R. J.; Rosenspire, K. C.; Jagoda, E.; Nanjappan, P.; Eckelman, W. C.; Nowotnik, D. P.; Nunn, A. D. Boronic acid adducts of technetium dioxime (BATO) complexes derived from quinuclidine benzilate (QNB) boronic acid stereoisomers: syntheses and studies of their binding to the muscarinic acetylcholine receptor. *Nucl. Med. Biol.* **1995**, *22*, 269−281.
(32) Meegalla, S. K.; Plössl, K.; Kung, M.-P.; Stevenson, D. A.; Liable-Sands, L. M.; Rheingold, A. L.; Kung, H. F. First example of a Tc-99m complex as a dopamine transporter imaging agent. *J. Am. Chem. Soc.* **1995**, *117*, 11037−11038.
(33) Madras, B. K.; Jones, A. G.; Mahmood, A.; Zimmerman, R. E.; Garada, B.; Holman, B. L.; Davison, A.; Blundell, P.; Meltzer, P. C. Technepine: a high affinity technetium-99m probe to label the dopamine transporter in brain by SPECT imaging. *Synapse* **1996**, *22*, 239−246.
(34) Carroll, F. I.; Abraham, P.; Lewin, A. H.; Parham, K. A.; Boja, J. W.; Kuhar, M. Isopropyl and phenyl esters of 3β-(4-substituted phenyl)tropane-2β-carboxylic acids. Potent and selective compounds for the dopamine transporter. *J. Med. Chem.* **1992**, *35*, 2497−2500.
(35) Oya, S.; Plössl, K.; Kung, M.-P.; Stevenson, D. A.; Kung, H. F. Small and neutral TcO(V) BAT, bisaminoethanethiol (N_2S_2) complexes for developing new brain imaging agents. *Nucl. Med. Biol.* **1996**, in press.
(36) Lever, S. Z.; Baidoo, K. E.; Mahmood, A. Structure proof of syn/anti isomerism in N-alkylated diaminedithiol (DADT) complexes of technetium. *Inorg. Chim. Acta* **1990**, *176*, 183−184.
(37) Mahmood, A.; Halpin, W. A.; Baidoo, K. E.; Swigart, D. A.; Lever, S. Z. Synthesis and characterization of N-ethyl-diaminedithiol oxotechnetate (V): a potential lung imaging agent. In *Technetium and Rhenium in Chemistry and Nuclear Medicine;* Nicolini, M., Bandoli, G., Mazzi, U., Eds.; Raven Press: New York, 1990; p 113.
(38) Wolff, J. A. Massachusetts Institute of Technology Thesis, MIT, MA, 1991.
(39) Kung, H. F.; Kim, H.-J.; Kung, M.-P.; Meegalla, S. K.; Plössl, K.; Lee, H.-K. Imaging of dopamine transporters in humans with technetium-99m TRODAT-1. *Eur. J. Nucl. Med.* **1996**, *23*, 1527−1530.
(40) Ell, P. J. Milestones [editorial]. *Eur. J. Nucl. Med.* **1996**, *23*, 1441.
(41) Alberto, R.; Schibli, R.; Egli, A.; Schubiger, P. A.; Herrmann, W. A.; Artus, G.; Abram, U.; Kaden, T. A. Metal carbonyl syntheses XXII. Low pressure carbonylation of $[MOCl_4]^-$ and $[MO_4]^-$: the technetium(I) and rhenium(I) complexes $[NEt_4]_2[MCl_3(CO)_3]$. *J. Organomet. Chem.* **1995**, *493*, 119−127.
(42) Kung, H. F.; Molnar, M.; Billings, J.; Wicks, R.; Blau, M. Synthesis and biodistribution of neutral lipid-soluble Tc-99m complexes that cross the blood-brain barrier. *J. Nucl. Med.* **1984**, *25*, 326−332.
(43) Kung, H. F.; Yu, C. C.; Billings, J.; Molnar, M.; Blau, M. Synthesis of new bis-aminoethanethiol (BAT) derivatives: possible ligands for Tc-99m brain imaging agents. *J. Med. Chem.* **1985**, *28*, 1280−1284.

JM960532J